Kinetics of Release of Particulate Solutes Incorporated in Cellulosic Polymer Matrices as a Function of Solute Solubility and Polymer Swellability. III. Moderately Soluble Solute

K. G. PAPADOKOSTAKI, M. E. HEROUVIM

Institute of Physical Chemistry, Demokritos National Research Center, 15310 Aghia Paraskevi, Athens, Greece

Received 2 August 2001; accepted 20 August 2001

ABSTRACT: Our previous investigation of the kinetics of release of simple particulate solutes of very low ($CaSO_4$ or $SrSO_4$) or very high aqueous solubility (NaCl) from cellulose acetate (CA) matrices (in the form of thin films) in contact with an eluant aqueous phase is here extended to a solute of moderate solubility ($CsNO_3$). Simultaneous measurement of the concurrent variation of the water content of the matrix revealed the occurrence of osmotically induced excess water uptake by the loaded matrix for all loads studied, as previously observed in the case of NaCl at lower loads. The resulting enhancement of solute release rate was considerable but much less than that generated by NaCl. Sorption and diffusion of the solute in the corresponding particle-depleted polymer matrices was also investigated. The results exhibited a pattern qualitatively very similar to that of NaCl but greatly attenuated in quantitative terms. These observations are in keeping with the relatively weak osmotic power of $CsNO_3$. A mechanism for osmotically induced enhancement of solute release rate previously formulated (in terms of the growth of zones of enhanced hydration of the polymer matrix surrounding the embedded solute particles) to account for NaCl release behavior observed at lower particle loads was found to be applicable here at all loads examined. The degree of hydration of the (neat) CA polymer matrix was also varied (by varying the conditions of film preparation or by wet thermal after-treatment of the as-prepared films) and its effect on $CsNO_3$ partition and diffusion coefficients was studied. The results provided the basic information needed for interpretation of the corresponding particle-depleted film data, in comparison with the previous ones for NaCl. It was thus shown that imbibed water was more homogeneously distributed in NaCl-depleted, than in $CsNO_3$-depleted, films. It was also observed that variation of the degree of polymer hydration affected primarily the rate, and only secondarily the kinetics, of particulate $CsNO_3$ release. © 2002 Wiley Periodicals, Inc. J Appl Polym Sci 84: 2028–2039, 2002; DOI 10.1002/app.10499

Key words: release kinetics; osmotic effect; swelling; cellulose acetate films; permeability

INTRODUCTION

Previous articles of this series focused on the kinetics of release of simple solutes of very low ($CaSO_4$ and $SrSO_4$)[1] and very high (NaCl)[2] aqueous solubility dispersed in the form of fine particles in a moderately hydrophobic cellulosic (cellulose acetate, abbreviated to CA) matrix, in contact with an eluting aqueous phase. A significant feature of this work was that release kinetics was correlated with both the concurrent variation of the water content of the matrix and the sorption

Correspondence to: K. G. Papadokostaki (kpapadok@chem.demokritos.gr).

Journal of Applied Polymer Science, Vol. 84, 2028–2039 (2002)

and diffusion properties of the particle-depleted matrix. Comparison of the latter properties with those of neat CA matrices of various degrees of hydration was shown to provide significant insight into the morphology of the particle-depleted matrix and ultimately into the mechanism of osmotically induced enhancement of release rate in the case of soluble solutes. Such osmotic mechanisms play an important role in practical applications such as monolithic controlled release devices, incorporating osmotically active solutes or excipients (e.g., [3–8]), or hydrothermal aging of polymeric composites (e.g., ref. [9]).

In view of the fact that the dispersed solute is immobile, its observed rate of release into the eluant phase should be governed (1) by the maximum amount of solute which can dissolve in the hydrated matrix under the prevailing conditions (represented by the saturation value C^0_{NS} of the concentration of dissolved solute C_{NS}, given here in g/cm^3 of the hydrated polymer matrix) and (2) by the mobility of this dissolved solute in the hydrated matrix, represented by the diffusivity D_N.

We consider a polymeric matrix in the form of a thin film of thickness $2l$, loaded initially with a total concentration of solute C_{NO} (expressed in the same units as C_{NS}) and immersed in a well-stirred infinite aqueous bath. Under conditions of (1) fast penetration of water into the matrix relative to solute transport; (2) instantaneous equilibrium between dispersed and dissolved solute in the matrix; and (3) $C_{NO} \gg C^0_{NS}$, the release process may be described by the well-known equation[1,10,11]

$$\frac{M_{Nt}}{M_{N\infty}} = \left(\frac{2D_N C^0_{NS} t}{l^2 C_{NO}}\right)^{1/2} \equiv \left(\frac{2P_N c^0_{NS} t}{l^2 C_{NO}}\right)^{1/2} \qquad (1)$$

where M_{Nt}, $M_{N\infty}$ denote the amount of solute released at times t and $t \to \infty$, respectively; $P_N = D_N K$ is the permeability coefficient; and the partition coefficient (assumed constant) $K = C_{NS}/c_{NS} = C^0_{NS}/c^0_{NS}$ characterizes the equilibrium between dissolved solute in the matrix and in aqueous solution (where the concentration c_{NS} and the corresponding saturation value c^0_{NS} are given in g/cm^3 of solution). Under the conditions specified above, the concentration profile of the solute between the middle of the film and either surface exposed to eluant takes the form of an inward moving sharp front, which divides an outer region fully depleted of dispersed solute ($C_N = C_{NS}$) from an inner region still practically fully loaded with solute ($C_N = C_{NO}$). Solute release then occurs essentially by diffusion of dissolved solute through the former region under a (very nearly constant) concentration gradient extending from $C_{NS} = C^0_{NS}$ at the sharp front to $C_{NS} = 0$ at the exposed surface of the film. Thus, P_N and D_N are characteristic of the particle-depleted matrix.

In the case of low-solubility solutes [the kinetic behavior of which conforms closely to eq. (1)], the particle-depleted film should be an exact replica of the particle-loaded one, except for the fact that the cavities vacated by the solute particles (occupying a volume fraction ϵ_N in the loaded matrix) are now filled with water. Thus,[1,2] the water content of these films (fractional volume ϵ_W) is made up of (1) water hydrating the polymer to an extent equal to that in the particle-loaded or neat film, under the same conditions, and occupying a fractional volume ϵ_{WP}; (2) water filling any air gaps left in the particle-loaded films as prepared (because of incomplete impregnation of the solute particles by the viscous polymer dope from which the film was cast; see experimental section), occupying a volume fraction ϵ_g; and (3) water replacing solute particles, as above, of volume fraction ϵ_N; for instance,

$$\epsilon_W = \epsilon_{WP} + \epsilon_g + \epsilon_N \qquad (2)$$

Because of the large difference of the permeabilities (P_{NM}, P_{NS}) of the solutes under study here in hydrated CA and in aqueous solution, respectively (P_{NS} exceeds P_{NM} by more than five orders of magnitude), the distribution in the polymer matrix of the additional imbibed water, represented by components 2 and 3 above, is of great importance. In particular, P_N should be greatly enhanced, if the said aqueous phase can provide continuous pathways through the polymer matrix.

Thus, at low particle loads ($\epsilon_N \lesssim 0.1$), where complete coating of solute particles with polymer was achieved (evidenced by $\epsilon_g = 0$),[1] P_N may be enhanced only marginally above P_{NM}, because imbibed water component 3 would be in the form of globules isolated from each other. Hence, the release process would be rate-controlled by solute transport in the hydrated CA matrix.[1] At higher particle loads, the encapsulation (impregnation) of solute particles with the polymer dope becomes increasingly incomplete. The appearance of imbibed water component 2 then increasingly bridges neighboring globules, thus building up

facile pathways for solute and leading to an observed enhancement of P_N far out of proportion to the value of ϵ_N (e.g., amounting to ca. four orders of magnitude above P_{NM} for $CaSO_4$ at $\epsilon_N \approx 0.4$).[1]

Another way of bridging the water globules dispersed in the particle-depleted film is to increase the degree of hydration of the matrix (imbibed water component 1), as exemplified by the hydrolysis of the CA matrix to cellulose in Part I.[1]

A very similar effect can be produced by the osmotic action of a water-soluble particulate solute (exemplified by NaCl in Part II). The view commonly held in this respect is that imbibed water in the polymer matrix is osmotically driven into the particle-containing cavities; the latter swell and the cavity wall finally fails mechanically under the resulting stress.[3–5] Neighboring cavities are thus bridged by cracks or breaches of the intervening wall and a permanent aqueous pore system is created in the particle-depleted matrix. This cavity–wall rupture mechanism of enhanced solute release is plausible at relatively high loads but could hardly be reconciled with our observation[2] of NaCl-induced enhancement of P_N by approximately two orders of magnitude over P_{NM}, at particle volume fractions as low as $\epsilon_N = 0.06$ (corresponding to unusually thick intercavity walls). This was accompanied by substantial amounts of temporary water uptake over and above that indicated by eq. (2), implying substantial excess hydration of the polymer itself.[2]

On the basis of this and other evidence, a new mechanism of osmotically enhanced release rate was formulated[2] in terms of zones of enhanced hydration (ZEH). These zones develop around the particle-containing cavities and fan out until they merge with those of neighboring cavities, thus creating continuous regions of enhanced polymer hydration, wherein solute diffusion can proceed much more rapidly. Thanks to the stiffness of the cellulosic chains, the ZEH persist to a substantial degree after all particulate solute in the relevant cavities has been released, as demonstrated by the observation that loss of osmotically induced excess water uptake continues long after the film has been completely depleted of solute. Furthermore, at the end of this prolonged deswelling period, and despite the fact that the amount of water left in the film conformed reasonably well to eq. (2), the value of P_N had declined by only one order of magnitude (i.e., still exceeded P_{NM} by one order of magnitude). This is consistent with the persistence of quite extensive bridging of solute-vacated cavities. On the other hand, the results of analysis of NaCl partition coefficient (K) data from neat and particle-depleted films, in conjunction with information from the literature on the dependence of K on imbibed water in neat films, were consistent with partial collapse of the said cavities.[2] Thus, it may be said that the morphology of the particle-depleted CA matrix bears an imprint of the ZEH.

In view of the interesting findings summarized above, it seemed worthwhile to fill in the picture which has emerged by a similar kinetic and structural study of the same polymer matrix loaded with a particulate solute of moderate solubility. $CsNO_3$, the aqueous solubility of which (0.144 mol/dm^3) is approximately four times less than that of NaCl, was selected for this purpose. This study was complemented by an investigation of the effect of the degree of hydration of the polymer, which was varied either by adjustment of the conditions of film preparation or by appropriate after-treatment of the as-prepared films.

EXPERIMENTAL

Preparation of CA Polymer Matrices

Films, in neat form (designated as type A; thickness $2l = 100–120$ μm) or loaded with various amounts of dispersed $CsNO_3$ (Alpha, Karlsruhe, Germany) particles (designated as type B; $2l = 260–385$ μm), were prepared from the same CA powder (Eastman Chemicals, Kingsport, TN, type CA-398-30), using exactly the same experimental technique and conditions as in Parts I and II (namely casting of a 20% CA solution in acetone, with the particles dispersed therein, on a glass plate, followed by solvent evaporation in a relatively humid environment for 2–3 days and subsequent evacuation for a similar period). These films are characterized by what we shall consider as a normal degree of hydration and are designated as type AN or BN.

Films of enhanced degree of hydration (characterized by lower crystallinity; see Fig. 1) were prepared by carrying out the solvent evaporation step in a low humidity environment (designated as type AL or BL). Films of a reduced degree of hydration (due to enhanced crystallinity and/or more compact amorphous phase)[15,16] were prepared by wet thermal treatment of films in water (for neat films, designated as type ANH) or in a saturated aqueous $CsNO_3$ solution (for loaded films, designated as type BNH), at 98°C for 3 h.

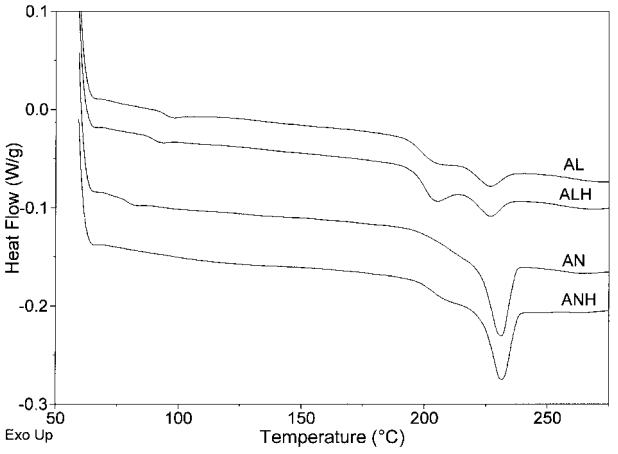

Figure 1 Typical DSC thermograms characteristic of neat CA films of type AL, AN, ALH, and ANH, prepared as described in the experimental section.

Films of type AL or BL were also subjected to wet heat treatment as above (designated ALH or BLH, respectively).

As in Part II, the sorption and diffusion properties of the corresponding particle-depleted films were also studied. These films are referred to as type C and further designated as CN, CL, CNH, or CLH, according to the type of the original loaded film (BN, BL, BNH, or BLH, respectively).

$CsNO_3$ (analytical reagent grade) particles of size ~ 5 μm (as closely similar as possible to that of the $CaSO_4$ and NaCl particles previously used[1,2]) were prepared by precipitation from aqueous solution with alcohol.

Experiments with Particle-Loaded (type B) Films

The amount of solute released from, and the amount of water imbibed by, loaded film specimens [initially conditioned at relative humidity (RH) = 0.40], were determined at 25°C, as a function of time, by the methods described in Part II.

Experiments with Neat (type A) or Particle-Depleted (type C) Films

Film specimens were first equilibrated at 25°C with 0.1 or 0.2 g/cm^3 aqueous $CsNO_3$ solutions and the desorption of solute after subsequent immersion in water was monitored to determine the relevant partition (K) and diffusion (D_N) coefficients, as described in Part II.[2] Equilibrium water uptake (C_W^0) was also measured as in Part II.

RESULTS AND DISCUSSION

Characteristics of Neat Films

Typical $CsNO_3$ sorption and transport properties of neat (type A) CA films of different degrees of polymer hydration are given in Table I and characteristic differential scanning calorimetric (DSC) thermograms (carried out on a TA Instruments MDSC model 2920 at a heating rate of 5°C/min) are shown in Figure 1. It will be noted that, as expected, the relevant permeability, partition, and diffusion coefficients (designated by P_{NM}, K_M, and D_{NM}, respectively) all follow the order AL > AN > ALH > ANH, which is also the order of increasing polymer hydration.

Effect of Solute Osmotic Power on the Kinetics of Particulate Solute Release from Matrices of Normal Degree of Hydration (BN films)

Figures 2-4 illustrate (on a $\sqrt{t}$ scale) the kinetics of solute release from, and concurrent variation of imbibed water in, films of normal degree of hydration loaded with $CsNO_3$ particles, in comparison with the corresponding results[2] for NaCl (and for $CaSO_4$ where possible[1]). The $CsNO_3$ loads were chosen to yield the same particle volume fraction ϵ_N as in the case of NaCl.[2]

The solute data (represented by squares in Figs. 2–4) are given in terms of the fractional amount of solute released $M_{Nt}/M_{N\infty}$. The data on imbibed water are given as fractional amounts (1) of total imbibed water $M_{Wt}/M_{W\infty}$ (represented by circles in Figs. 2–4) and (2) of imbibed water other than that replacing particulate solute $M'_{Wt}/M'_{W\infty}$ (i.e., $M'_{Wt} = M_{Wt} - M_{Nt}d_N$, where d_N is the density of solid solute) and hence consisting only

Table I Water Content (C_W^0, on dry CA basis) and $CsNO_3$ Permeability (P_{NM}), Partition (K_M), and Diffusion (D_{NM}) Coefficients Typical of Neat (type A) CA Films

Film Type	C_W^0 (g/g)	$P_{NM} \times 10^8$ (cm^2 s^{-1})	K_M	$D_{NM} \times 10^9$ (cm^2 s^{-1})
AL[a]	0.17_9	3.8	0.16_0	2.4
AN[b]	0.15_4	1.2	0.12_0	1.0
ALH[c]	0.14_8	0.83	0.11_1	0.75
ANH[d]	0.13_4	0.49	0.097	0.50

[a] Lower crystallinity, higher hydration.
[b] Normal crystallinity and hydration.
[c] AL subjected to wet heat treatment.
[d] AN subjected to wet heat treatment.

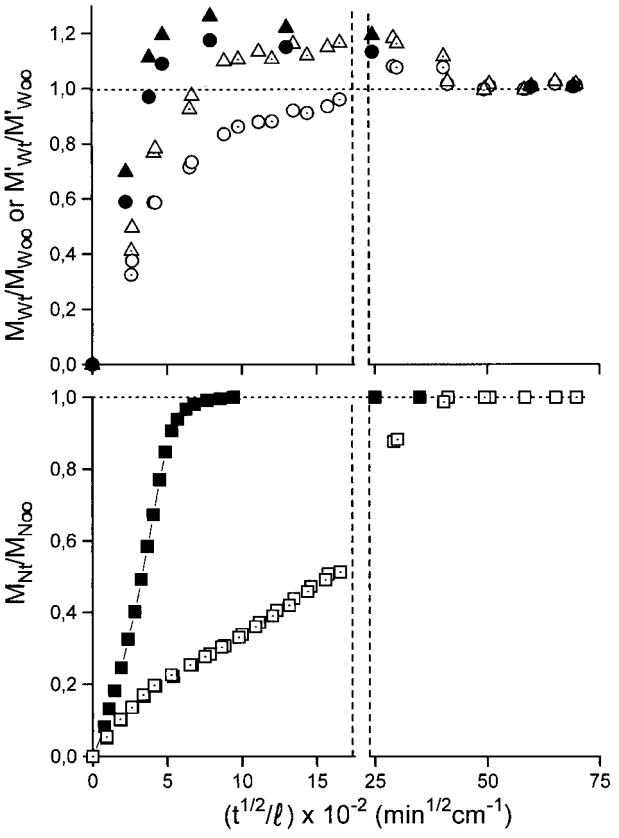

Figure 2 Kinetic curves of fractional solute release ($M_{Nt}/M_{N\infty}$; □, ■) from, and concurrent variation of total imbibed water ($M_{Wt}/M_{W\infty}$; ○, ●), or of water of hydration of the polymer ($M'_{Wt}/M'_{W\infty}$; △, ▲) in CA films (~ 300 μm thick) of normal degree of hydration (type BN) loaded with $CsNO_3$ particles (open points), in comparison with corresponding results for NaCl (filled points)[2]: $\epsilon_N = 0.06$.

of the imbibed water components 1 and 2 defined in the introductory section (represented by triangles in Figs. 2–4). These quantities are calculated on the basis of the appropriate amount of imbibed water ($M_{W\infty}$ or $M'_{W\infty}$, respectively) remaining in the particle-depleted matrix after the release experiment was completed and sufficient extra time (usually 3–7 days) was allowed for the water content of the depleted matrix to stabilize. The latter precaution is important, because of the slow loss of osmotically induced excess water uptake, already referred to in the introduction and illustrated in Figures 2–4.

As shown in Figures 2 and 3, the $CsNO_3$ release curves for lower loads exhibit an extensive, sensibly linear middle portion, which is in conformity to eq. (1) but extrapolates to a finite intercept $M_{Nt}/M_{N\infty} < 0.1$ at $t = 0$, because of a brief initial period of enhanced release rate. In this respect, they resemble very closely the corresponding low-load $CaSO_4$ release curves (cf. the two lower release curves in Fig. 1 of Part I). This phenomenon was investigated in Part I and shown to be attributable to the fact that solute particles located at, or very near, the film surfaces are less well coated with polymer and hence are more exposed to eluant. It is not observed at high loads (where particles everywhere in the matrix are not fully coated with polymer; cf. the upper release curve in Fig. 1 of Part I) or in highly hydrated polymer matrices, whether the high degree of hydration is innate (as in cellulose-$CaSO_4$; cf. Fig. 3 of Part I) or osmotically induced (as in the case of CA-NaCl illustrated in Figs. 2 and 3 here).

The P_N values (denoted by P_{NB} to make clear that they pertain to type B films) determined from the linear parts of the appropriate curves are shown in Table II (note that P_{NB} for NaCl at $\epsilon_N = 0.06$ was deduced from the initial part of the relevant curve and is, therefore, a conservative estimate, because of a significant tendency of the slope of the said curve to rise at a later stage of the release process[2]). In the case of $\epsilon_N = 0.22$ (illustrated in Fig. 4), the $CsNO_3$ release curves exhibit distinct convex upward curvature, implying a tendency of P_{NB} to decrease in the course of the experiment. This point will be considered further below. A mean effective value of P_{NB} has been recorded in Table II. It can be seen that P_{NB} for $CsNO_3$ is markedly lower than that of NaCl and much higher than that of $CaSO_4$.

As shown in Table I, the solutes under discussion also exhibit marked differences in permeability (P_{NM}) through neat CA (type A) films, although the order is different, namely $CsNO_3 >$ NaCl $> CaSO_4$, which is the same as in aqueous solution. The primacy of $CsNO_3$ here is attributable to its lower dielectric exclusion from the hydrophobic CA matrix and its lower degree of hydration in aqueous solution, respectively.

In view of the aforementioned differences in P_{NM}, it is of interest to examine the behavior of the normalized quantities P_{NB}/P_{NM} (see Table II), which represent the enhancement of permeability associated with increases in particle fractional volume ϵ_N and solute osmotic power. As expected, $CsNO_3$ occupies an intermediate position between $CaSO_4$ (representing effectively zero osmotic effect) and the spectacular permeability enhancement caused by NaCl, which can only be osmotically induced via ZEH at $\epsilon_N \lesssim 0.1$ (where effec-

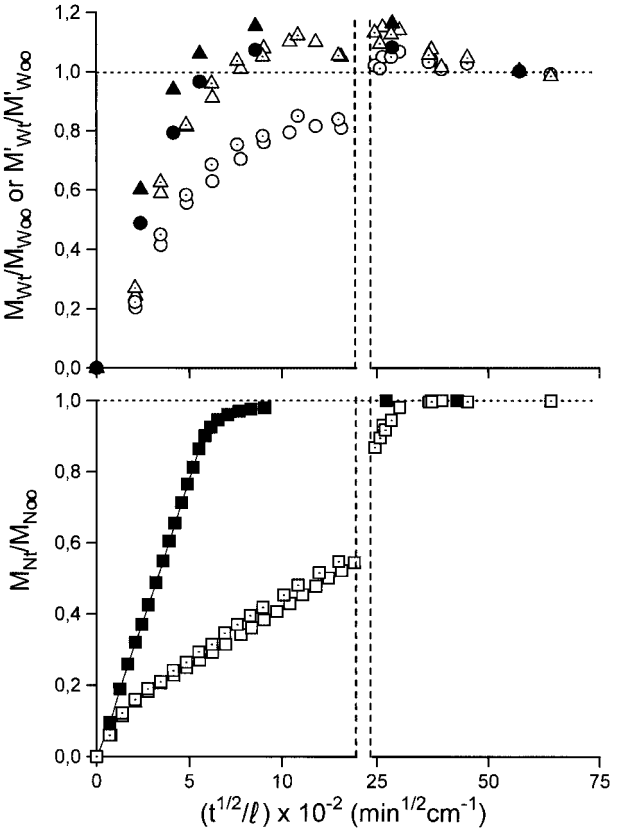

Figure 3 Solute release kinetic curves from, and concurrent variation of imbibed water in, CA films of normal hydration loaded with $CsNO_3$ particles (open points), in comparison with corresponding results for NaCl (filled points),[2] as in Figure 2 but for $\epsilon_N = 0.11$.

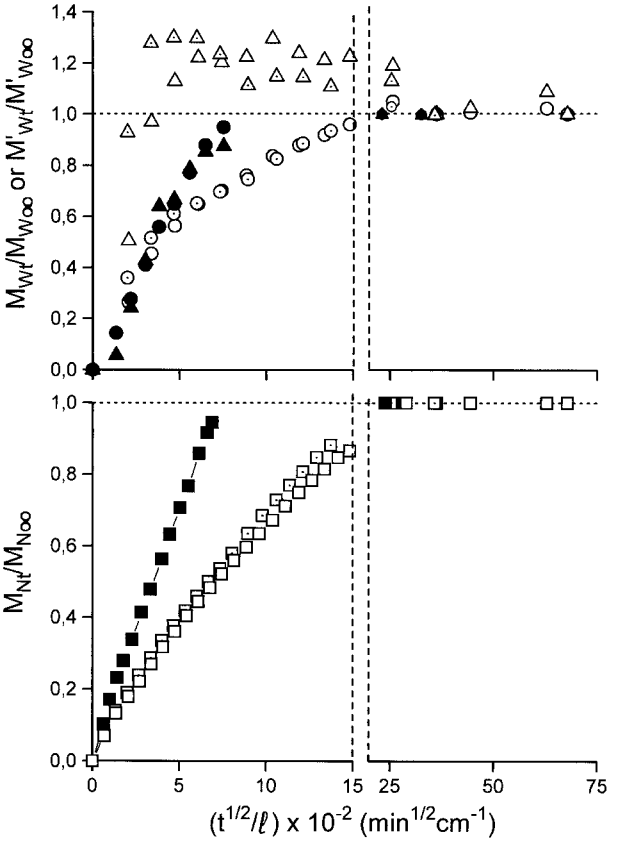

Figure 4 Solute release kinetic curves from, and concurrent variation of imbibed water in, CA films of normal hydration loaded with $CsNO_3$ particles (open points), in comparison with corresponding results for NaCl (filled points),[2] as in Figure 2 but for $\epsilon_N = 0.22$.

Table II Experimental Permeabilities of $CsNO_3$ Particle-Loaded Films of Normal Polymer Hydration (type BN), in Comparison with Analogous Data for NaCl and $CaSO_4$ and with Values Calculated from eq. 4 (see text)

Solute	ϵ_N	$P_{NB} \times 10^9$ ($cm^2\ s^{-1}$)	P_{NB}/P_{NM} Expt.	P_{NB}/P_{NM} Eq. 4
$CsNO_3$	0.06_0	0.54	4.50	1.22
	0.11_6	2.0	17.0	1.53
	0.22_4	7.3	61.0	3.05
NaCl	0.06_1	10	240	1.22
	0.11_5	15	360	1.53
	0.22_3	21	500	3.02
$CaSO_4$	0.09_1	0.0057	1.38[a]	1.38
	0.22_8	1.4	350	3.16

[a] Estimated.

tively complete coating of solute particles with polymer may be safely assumed[1,2]).

The view that a similar release-acceleration mechanism is operative in the case of $CsNO_3$ is supported by the presence, here too, of substantial amounts of osmotically induced excess water uptake (as shown in Figs. 2 and 3). The fact that the resulting fractional gain in permeability is much less than that shown by NaCl, especially at $\epsilon_N = 0.06$ (see Table II), is attributable to the expected generally smaller osmotically induced enhancement of polymer hydration and perhaps to less extensive ZEH also. The latter eventuality is supported by the fact that an increase of ϵ_N from 0.06 to 0.11 resulted in a substantial rise of P_{NB}/P_{NM} for $CsNO_3$ but only in a rather marginal one in the case of NaCl. On the other hand, it may seem surprising that similar maximum amounts of excess imbibed water are shown in Figures 2 and 3 for NaCl and $CsNO_3$. One should bear in

mind, however, that one is here looking at the amounts of imbibed water present in the whole matrix. As illustrated in Figure 2 of Part II (as well as by the times at which the relevant $M'_{Wt}/M'_{W\infty}$ curves in Figs. 2 and 3, which essentially represent water hydrating the polymer, exceed unity), the rate of water penetration into the matrix is comparable with that of NaCl release but much faster than that of $CsNO_3$ release. Accordingly, the inner fully loaded region of the film soon becomes fully hydrated in the case of $CsNO_3$ (hence, apart from an initial period, one is observing an osmotic effect extending over the whole of this inner film region) but remains only weakly hydrated in the case of NaCl (hence, a strong osmotic effect is actually operating only over a narrow zone of the inner region next to the sharp boundary). Thus, one should, more properly, compare the amount of excess imbibed water present in each case at the end of the relevant release experiment.

A rather different picture emerges when the solute load is increased to $\epsilon_N = 0.22$ (see Fig. 4 and Table II); there is a substantial increase in P_{NB}/P_{NM} for $CsNO_3$, paralleled by a much less marked one for NaCl but a very marked one for $CaSO_4$. As explained in Part I (see also the introduction), the sharp rise of P_{NB}/P_{NM} for $CaSO_4$ (amounting to more than two orders of magnitude above what could be theoretically expected for fully coated solute particles, represented by the corresponding value of P^0_N/P_{NM} calculated as explained below) reveals the presence of facile solute transport pathways, which could only be in the form of water-filled pores. However, the resulting absolute value of P_{NB} for $CaSO_4$ is still quite modest. Taking into account the fact that $CsNO_3$ diffuses in aqueous solution ($P_{NS} \cong 2.0 \times 10^{-5}$ cm^2 s^{-1}) nearly twice as fast as $CaSO_4$ ($P_{NS} \cong 0.9 \times 10^{-5}$ cm^2 s^{-1}), this effect can account for less than half the corresponding value of P_{NB} for $CsNO_3$. This discrepancy is accounted for by the simultaneous operation of an osmotic ZEH mechanism (evidenced by the substantial amounts of excess imbibed water observed) in the case of $CsNO_3$ (see Fig. 4). The absence of any corresponding excess imbibed water in the case of NaCl (where the aforementioned incomplete coverage of the embedded particles with polymer could account for less than one tenth of the recorded value of P_{NB}) is remarkable; it suggests that a cavity–wall rupture osmotic mechanism (which, as explained in Part II, is not associated with excess water uptake) becomes operative at this higher fractional particle volume in the case of NaCl.

Table III Experimental Permeabilities of Particle-Depleted Films (type CN) Corresponding to the BN Films of Table II

Solute	ϵ_N	$P_{NC} \times 10^9$ (cm^2 s^{-1})	P_{NB}/P_{NC}	P_{NC}/P_{NM}
$CsNO_3$	0.06_0	0.27	2.0	2.2
	0.11_6	0.65	3.1	5.4
NaCl	0.06_1	0.35	29	8.3
	0.11_5	1.0	15	24

Reference to the corresponding particle-depleted (type C) film permeabilities P_{NC} (see Table III) reveals a pattern for $CsNO_3$ qualitatively very similar to that for NaCl (note that $P_{NC} = P_{NB}$ for $CaSO_4$). In particular, we note that $P_{NB}/P_{NC} > 1$ and $P_{NC}/P_{NM} > 1$, but (not unexpectedly) the values of these quantities pertaining to $CsNO_3$ deviate from unity much less than those of NaCl. The former quantity provides a measure of the extent to which the particle-depleted matrix has relaxed from the state of excess hydration osmotically induced during the release experiment. The tendency of P_{NB}/P_{NC} to increase with ϵ_N (shown in Table III), in conjunction with the relatively long duration of the $CsNO_3$ experiments, suggests that the tendency of P_{NB} for $CsNO_3$, at $\epsilon_N = 0.22$, to decline during the release experiment (noted above in Fig. 4) may well reflect the occurrence of this deswelling relaxation process. On the other hand, the values of P_{NC}/P_{NM} may be compared with those predicted by the simple forms of the Maxwell and Böttcher equations (given in Parts I and II)[1,2] for a binary medium consisting of a disperse phase of permeability P_{NS} (water globules replacing solute particles) embedded in a continuous phase of permeability P_{NM} (hydrated polymer matrix) for the case of $P_{NS}/P_{NM} \gg 1$ and low ϵ_N, namely

$$\frac{P_N}{P_{NM}} = \frac{1 + 2\epsilon_N}{1 - \epsilon_N} \tag{3}$$

$$\frac{P_N}{P_{NM}} = \frac{1}{1 - 3\epsilon_N} \tag{4}$$

respectively. As discussed in Part I, P_N/P_{NM} for a random dispersion of individual globules should lie between the lower and upper limits set by eqs.

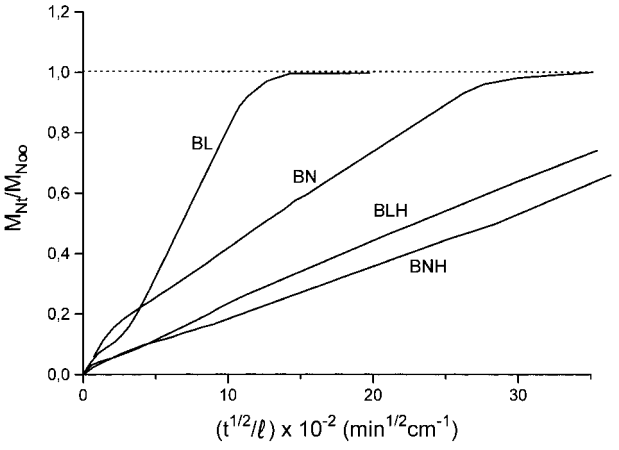

Figure 5 Typical kinetic curves of solute release from CA films of different degrees of hydration (type BL, BN, BLH, BNH) carrying the same load of $CsNO_3$ particles ($\epsilon_N = 0.11$).

(3) and (4), respectively. The values derived from eq. (4) (denoted by P_N^0/P_{NM} and shown in Table II) are considerably lower than the experimental P_{NC}/P_{NM} ones for $CsNO_3$ (shown in Table III) in all cases; thus confirming the presence of $CsNO_3$-induced morphological changes in the polymer matrix similar to the much more pronounced ones produced by the osmotic action of NaCl.

Effect of Polymer Hydration on the Kinetics of Release of Particulate $CsNO_3$

Typical kinetics of particulate $CsNO_3$ release are given (on a $\sqrt{t}$ scale) in Figure 5 for films of different degrees of hydration (types BL, BN, BLH, and BNH) carrying the same load (corresponding to $\epsilon_N = 0.11$). After initial stages, which are more pronounced in BN and BL films (in keeping with the fact that solute at or very near the surface tends to be removed by the wet heat after treatment), the release curves remain linear over long periods. Therefore, polymer hydration primarily affects the release rate.

The resulting P_{NB} values are listed in Table IV together with the P_{NC} ones pertaining to the corresponding particle-depleted films. Both these sets of permeabilities (for given ϵ_N) follow the order of increasing hydration previously noted for P_{NM} (Table I), except in cases where the relevant P_{NM} values are not very different (cf. films BN and BLH). The general pattern of behavior of P_{NB}/P_{NM}, P_{NC}/P_{NM}, and P_{NB}/P_{NC} noted previously is also not substantially affected. It will be noted in particular that the values of P_{NC}/P_{NM} exceed, in all cases, those calculated from eq. (4) (P_N^0/P_{NM} listed in Table II).

Dependence of the Solute Partition Coefficient on Polymer Hydration in Neat and Particle-Depleted Films

A useful aspect of the study of the dependence of the partition coefficient K_M on polymer hydration (C_W^0) is that it can provide a norm for quasi-homogeneous distribution of imbibed water in the polymer, against which the partition coefficients of particle-depleted films may be compared. The norm used for this purpose in Part II was provided by the NaCl partition data of Lonsdale et al.,[12] who varied C_W^0 by using neat films of CA of various degrees of acetylation. Here, this has been done, as indicated in the experimental section, by modifying the CA matrix physically, notably by enhancing or reducing the degree of crystallinity and/or amorphous structure compaction (note, incidentally, that variation of the degree of acetylation is also accompanied by such structural changes). Both these kinds of posttreatment are likely to affect other CA characteristics as

Table IV Permeabilities of $CsNO_3$ Loaded (type B), and Corresponding Particle-Depleted (type C), Films of Different Polymer Hydration

Film Type	ϵ_N	$P_{NB} \times 10^9$	$P_{NC} \times 10^9$	P_{NB}/P_{NM}	P_{NC}/P_{NM}	P_{NB}/P_{NC}
BL/CL	0.06_0	3.2	1.8	8.4	4.6	1.7
	0.11_6	9.3	4.1	25	10.2	2.3
BN/CN	0.06_0	0.54	0.27	4.5	2.2	2.0
	0.11_6	2.0	0.65	17	5.4	3.1
BLH/CLH	0.06_0	0.57	0.39	6.9	4.7	1.5
	0.11_6	0.83	0.65	10	7.8	1.3
BNH/CNH	0.06_0	0.22	0.12	4.6	2.5	1.8
	0.11_6	0.50	0.31	10	6.5	1.6

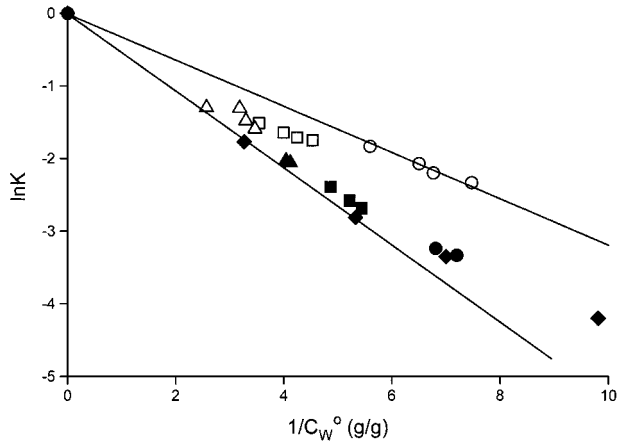

Figure 6 Dependence of $CsNO_3$ (open points) and NaCl (filled points) partition coefficients K on the water content of neat (○, ●) and particle-depleted ($\epsilon_N = 0.06$, □, ■; and $\epsilon_N = 0.11$, △, ▲) films, in conjunction with the NaCl data of Lonsdale et al.[12] (◆) based on CA neat films of different degrees of acetylation. The lines represent the behavior of K_M according to eq. (5) with $\beta_M = 0.318$ ($CsNO_3$), 0.530 (NaCl).

well, but hopefully not in a way that would invalidate the correlation of K (and of D_{NM} also, see below) with C_W^0. As will be seen in the following subsection, this expectation was justified *ex post facto*.

As shown in Figure 6, the $CsNO_3$ partition coefficient of neat CA films conforms fairly well to the relation

$$K_M = \exp(-\beta_M/C_W^0) \tag{5}$$

extrapolating to the physically correct limit of $K_M = 1$, at $C_W^0 \to \infty$. The alternative partition coefficient parameter k_s used in Part II also gave a similar linear semilog plot; which, however, did not extrapolate to the above limit.

Accordingly, treatment of the present $CsNO_3$ data on particle-depleted films was based on K and, for comparison purposes, the same treatment was applied to the NaCl data for neat and particle-depleted films of Part II. As shown in Figure 6, the K_M data of Lonsdale et al.[12] conform acceptably to eq. (5) in the region of $C_W^0 = 0.18$–0.5 g/g ($1/C_W^0 = 2$–5.5), which is of interest here (even though this is not so for the data at lower C_W^0).

The K data for particle-depleted films in Figure 6 exhibit deviations from the appropriate K_M line, which are substantial and negative in the case of $CsNO_3$, and small and positive, in the case of NaCl. To understand these results properly, a quantitative investigation of the theoretically expected behavior is required.

We consider that the particle-depleted film is made up of (1) a hydrated polymer phase, consisting of masses M_{SHP} of solute, M_P of polymer, and M_{WH} of imbibed water, occupying a volume $V_{HP} = (M_P + M_{WH})/d_{HP}$, and characterized by partition coefficient $K_{HP} = M_{SHP}/V_{HP}c_{NS}$ and (2) an aqueous phase consisting of mass M_{SW} of solute, mass $(M_W - M_{WH})$ of water (where M_W is the total mass of imbibed water), volume $V_{WS} = (M_W - M_{WH})/d_{WS}$ and characterized by a partition coefficient $K_W = M_{SW}/V_{WS}c_{NS}$, which is unity if the said aqueous phase is identified with bulk solution. We then have

$$\begin{aligned} K &= \frac{M_{SHP} + M_{SW}}{(V_{HP} + V_{WS})c_{NS}} \\ &= \frac{\frac{1}{d_{HP}}(M_P + M_{WH})K_{HP} + \frac{1}{d_{WS}}(M_W - M_{WH})K_W}{\frac{1}{d_{HP}}\left(1 + \frac{M_{WH}M_W}{M_W M_P}\right) + \frac{1}{d_{WS}}(M_W - M_{WH})} \\ &= \frac{(1 + xC_W^0)K_{HP} + (1 - x)C_W^0 K_W d_{HP}/d_{WS}}{(1 + xC_W^0) + (1 - x)C_W^0 d_{HP}/d_{WS}} \end{aligned} \tag{6}$$

where $C_W^0 = M_{WH}/M_P$ g/g; $x = M_{WH}/M_W$; $d_{HP}/d_{WS} \cong 1.3$ for the system under consideration; $K_{HP} = K_M(xC_W^0) = \exp(-\beta_M/xC_W^0)$; and $\beta_M = 0.318$ ($CsNO_3$) or 0.530 (NaCl) are the values derived from the respective linear plots of Figure 6. Thus, increasingly homogeneous distribution of imbibed water is indicated by $x \to 1$ and maximum degree of inhomogeneity, at given x, is obtained when $K_W = 1$.

Realistic model computations with eq. (6) have been performed for $K_W = 1$, using the above values of β_M, over the water content range of $C_W^0 = 0.125$–0.5 g/g, for $x = 0.2$–1, where $x \approx 0.45$–0.70 is the range corresponding to the particle-depleted film data appearing in Figure 6. The results obtained are shown in Figure 7. They confirm that the behavior of K is quite variable and should, therefore, be mapped out before making any attempt to interpret the data. Under our experimental conditions, substantial negative deviations from the appropriate K_M line for $CsNO_3$, as well as corresponding positive deviations in the case of NaCl, are duly predicted. However, it is difficult to quantify the difference in the behavior exhibited by the $CsNO_3$ and NaCl data, particu-

larly in view of the marked variability of the predicted divergence from the K_M line, as a function of x and C_W^0, in the latter case. Nevertheless, it is still possible to say, on the basis of Figure 7, that the NaCl-depleted film data indeed lie relatively closer to the relevant K_M line (and hence to the quasi-homogeneous imbibed water distribution represented by the said line) than the $CsNO_3$ ones.

Dependence of Solute Diffusion Coefficient on Polymer Hydration in Neat and Particle-Depleted Films

As shown in Part II, the dependence of D_{NM} for NaCl on the hydration of the CA matrix, which emerges from the data of Lonsdale et al.[12] (based on neat CA films of different degrees of acetylation), may be interpreted reasonably well in terms

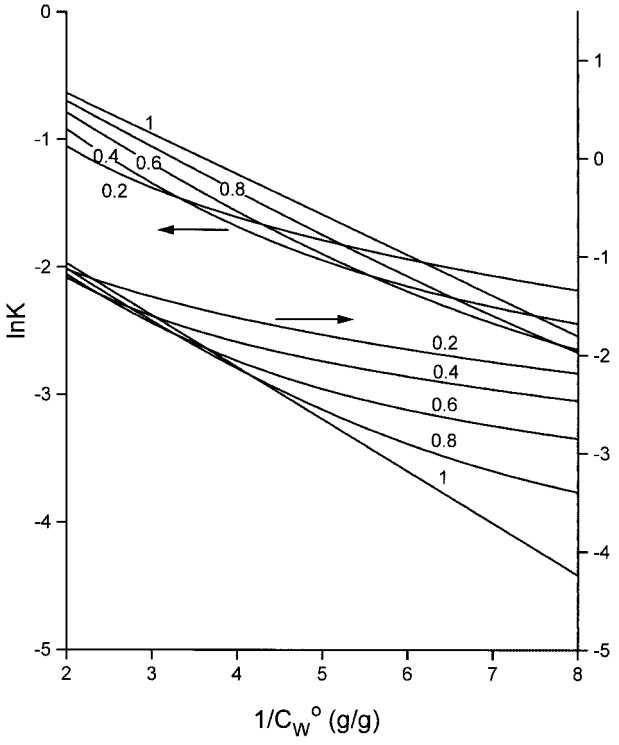

Figure 7 Predicted behavior of $CsNO_3$ (upper curves) and NaCl (lower curves) partition coefficients K, calculated by eq. (6), for a model medium simulating a particle-depleted CA matrix of total water content C_W^0 , a fraction x of which hydrates the polymer and the remainder is identified with bulk solution (see text for details). Numbers on curves are values of x. The ranges of practical interest here are $1/C_W^0 \approx 2$–4.5 ($CsNO_3$) and 4.0–5.5 (NaCl) and $x \approx 0.45$–0.7. The lines for $x = 1$ represent the behavior of K_M.

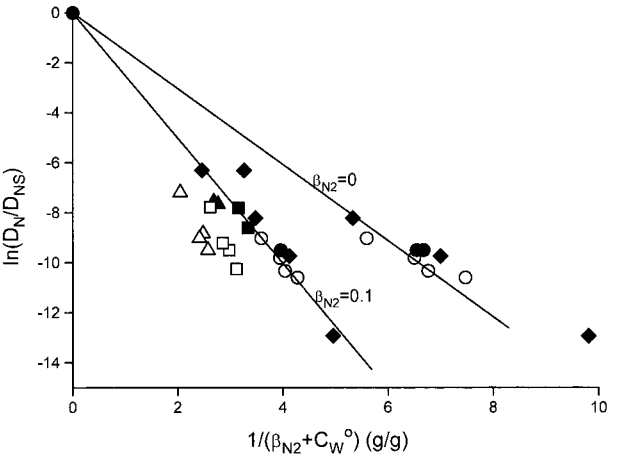

Figure 8 Dependence of the diffusion coefficients of $CsNO_3$ (open points) and NaCl (filled points) in CA (normalized with respect to the appropriate aqueous diffusion coefficients, D_{NS}) on the water content of neat (○, ●) and particle-depleted ($\epsilon_N = 0.06$, □, ■; $\epsilon_N = 0.11$, △, ▲) films, in conjunction with the NaCl data of Lonsdale et al.[12] based on CA neat films of different degrees of acetylation (♦). The lines represent the behavior of D_{NM}/D_{NS} according to eq. (7), with (a) $\beta_{N2} = 0$, $\beta_{N1} = 1.50$, or (b) $\beta_{N2} = 0.1$, $\beta_{N1} = 2.51$; following the simpler and more elaborate free-volume theories of Yasuda et al.[13,14]

of the equation of Yasuda et al.[13,14] (D_{NS} is the corresponding aqueous diffusion coefficient which is equal to P_{NS} referred above)

$$D_{NM} = D_{NS} \exp\left(-\frac{\beta_{N1}}{\beta_{N2} + C_W^0}\right) \qquad (7)$$

with $\beta_{N1} = 1.92$ g/g and $\beta_{N2} = 0.05$ g/g (see Fig. 6 of Part II). However, these data allow considerable latitude in deciding the best fitting value of β_{N2}, because of significant scatter in the aforementioned data of Lonsdale et al.[12] Our own neat-film diffusion results of Table I are fitted best by $\beta_{N2} = 0.1$ g/g. As shown in Figure 8, this value of β_{N2} also fits the Lonsdale et al. data to a degree comparable with that shown in Figure 6 of Part II. A significant point to note here is the close agreement between the aforementioned two independent sets of neat film data, which emerges in Figure 8. This is remarkable in view of the very different modification of the CA matrix underlying the variation of C_W^0 in these two cases (as discussed in the preceding subsection).

On the other hand, the close similarity of the diffusion behavior of $CsNO_3$ and NaCl, also im-

plied by the neat film data, is, of course, expected and permits direct comparison of the magnitude of the deviations from the neat film line exhibited by the particle-depleted film D_N values. We find that the said deviations (1) increase with increasing ϵ_N (for both $CsNO_3$- and NaCl-depleted films), as expected, in view of the rising amount of nonhomogeneously distributed imbibed water and (2) are more pronounced (for a given ϵ_N) for $CsNO_3$-depleted than for NaCl-depleted films, thus confirming the indication furnished by the corresponding partition coefficient data (see preceding subsection) that imbibed water is more homogeneously distributed in the latter films.

CONCLUSIONS

The particulate $CsNO_3$ release data relating to CA matrices of normal degree of hydration (designated as type N) presented here complement those of $CaSO_4$ and NaCl previously reported,[1,2] in a way that enables us to follow the rate-enhancing effect of progressively increasing solute osmotic power, for various solute volume fractions (ϵ_N) in the particle-loaded CA matrix. For this purpose, the relevant rate parameter P_{NB}, namely the permeability of the particle-depleted region of the film during the release experiment, defined by eq. (1), is used in the normalized form P_{NB}/P_{NM} to allow for the different permeabilities P_{NM} exhibited by these solutes in the neat polymer matrix.

In the absence of significant osmotic effects, represented by the case of $CaSO_4$, P_{NB}/P_{NM} increases with ϵ_N above unity only marginally, as long as the solute particles embedded in the loaded matrix are fully coated with polymer and the resulting water globules in the particle-depleted matrix are, therefore, isolated from each other. This appears to be so at $\epsilon_N \lesssim 0.1$ (evidenced by a measured volume fraction of air gaps, which fill with water in the hydrated loaded matrix, ϵ_g, equal to zero). At $\epsilon_N = 0.22$, we find $\epsilon_g > 0$, showing the presence of imbibed water bridging individual globules. The resulting sharp rise of P_{NB}/P_{NM} (by two orders of magnitude over what would be appropriate for a dispersion of isolated globules) is consistent with the formation of some continuous aqueous pathways through the CA matrix at this point. This effect is, of course, intensified with further rise of ϵ_N.

At the other extreme, the osmotic action of NaCl, put in evidence by the presence of substantial excess water uptake (which persists to a large extent in the depleted film region thanks to the stiffness of the cellulosic polymer chains) generates an even steeper rise of P_{NB}/P_{NM}, at ϵ_N as low as 0.06, by the ZEH mechanism referred to above and described in detail in Part II. The ZEH at this point apparently develop to such an extent that the further increase of ϵ_N to 0.11 entails only a relatively small further rise in P_{NB}/P_{NM}.

The same ZEH mechanism seems to be operative in the case of $CsNO_3$, except for the fact that its effect is far less marked, due to weaker and probably also less extensive ZEH, evidenced by the fact that $CsNO_3$ (in contrast to NaCl) exhibits a steady rise in P_{NB}/P_{NM} with increasing ϵ_N. The ZEH mechanism persists at $\epsilon_N = 0.22$, as shown by the continuing presence of substantial osmotically induced excess water uptake (and the fact that the incomplete particle encapsulation effect noted in the corresponding case of $CaSO_4$ can account only in part for the observed rise in P_{NB} for $CsNO_3$). On the other hand, NaCl, at $\epsilon_N = 0.22$, exhibits once again a relatively small further rise in P_{NB}/P_{NM} but no osmotically induced excess water uptake, suggesting that, at this ϵ_N, the walls of the particle-containing cavities are sufficiently thin for a cavity wall rupture mechanism to become possible for NaCl but not for $CsNO_3$.

The study of sorption and diffusion of solute in particle-depleted CA matrices of $\epsilon_N = 0.06$ and $\epsilon_N = 0.11$ gave results exhibiting a pattern qualitatively very similar to that of the corresponding NaCl data but greatly attenuated in quantitative terms (as expected), thus confirming the similarity of the release rate-enhancing osmotic mechanism operating in these two cases.

The above work was extended by the use of CA matrices of enhanced (type L) or reduced (type NH and LH) degree of hydration, prepared by varying the physical condition of the CA matrix, as described in the experimental section (in contrast to the approach of Lonsdale et al.,[12] who used CA matrices of different degrees of acetylation for this purpose).

The results obtained showed, on one hand, that variation of the degree of polymer hydration affects primarily the rate, and only secondarily the detailed kinetic behavior, of particulate $CsNO_3$ release.

On the other hand, study of the effect of varying polymer hydration on the $CsNO_3$ partition and diffusion coefficients in neat CA films gave results which conformed to eqs. (5) and (7), respectively, and furnished the basic information

needed for the comparative interpretation of the behavior of the corresponding $CsNO_3$ and NaCl data pertaining to particle-depleted films. The results of this data analysis (1) show that the widely different methods of varying the degree of polymer hydration used by Lonsdale et al. and by ourselves yield gratifyingly concordant results and (2) strongly suggest that imbibed water tends to be more homogeneously distributed in NaCl-depleted than in $CsNO_3$-depleted CA matrices, in line with the intuitive expectation that the stronger osmotic effect in the former case will leave a correspondingly more marked imprint on the morphology of the CA matrix.

The award of a scholarship to M.E.H. under the postgraduate program in "Polymer Science and its Applications" at the University of Athens is gratefully acknowledged.

REFERENCES

1. Papadokostaki, K. G.; Petropoulos, J. H.; Amarantos, S. G. J Appl Polym Sci 1998, 67, 277.
2. Papadokostaki, K. G.; Petropoulos, J. H.; Amarantos, S. G. J Appl Polym Sci 1998, 69, 1275.
3. Amsden, B. G.; Cheng, Y.-L.; Goosen, M. F. A. J Controlled Release 1994, 30, 45.
4. Amsden, B. G.; Cheng, Y.-L. J Controlled Release 1994, 31, 21.
5. Schirrer, R.; Thepin, P.; Torres, G. J Mater Sci 1992, 27, 3424.
6. Amsden, B. G.; Cheng, Y.-L. J Controlled Release 1995, 33, 99.
7. Dordunoo, S. K.; Octaba, A. M. C.; Hunter, W.; Min, W.; Cruz, T.; Burt, H. M. J Controlled Release 1997, 44, 87.
8. Catellani, P. L.; Colombo, P.; Peppas, N. A.; Santi, P.; Bettini, R. J Pharm Sci 1998, 87, 726.
9. Gautier, L.; Mortaigne, B.; Bellenger, V.; Verdu, J. Polymer 2000, 41, 2481.
10. Crank, J. The Mathematics of Diffusion, 2nd ed.; Clarendon Press: Oxford, U.K., 1975; Chapter 13.
11. Higuchi, T. J Pharm Sci 1961, 50, 874.
12. Lonsdale, H. K.; Merten, U.; Riley, R. L. J Appl Polym Sci 1965, 13, 1341.
13. Yasuda, H.; Lamaze, C. E.; Ikenberry, L. D. Macromol Chem 1968, 118, 19.
14. Yasuda, H.; Lamaze, C. E.; Peterlin, A. J Polym Sci, Part A: Poly Chem 1971, 9, 1117.
15. Malladi, D. P.; Scherrer, J. R.; Kint, S.; Bailey, G. F. J Membr Sci 1984, 19, 209.
16. Scherrer, J. R.; Bailey, G. F.; Kint, S.; Young, R.; Malladi, D. P.; Belton, B. J Phys Chem 1985, 89, 312.